Table 1: Stratigraphy and average rock properties (after Hunfeld et al. 2021) used for backstripping and decompaction.

Lithostratigraphic Unit	**Average Rock Type**	**Initial Porosity (%)**	**Depth Coefficient (km^{-1})**	**Grain density g/cm^3**	**Young Modulus (MPa)**	**Poisson Ratio**
Upper North Sea Group	Sandstone	0.49	0.27	2.65	15000	0.29
Middle and Lower North Sea Group	Sandstone	0.49	0.27	2.65	15000	0.29
Chalk Group	Limestone	0.70	0.71	2.75	37500	0.32
Rijnland Group	ShalySand	0.56	0.39	2.68	23750	0.3
Schieland, Scruff and Niedersachsen Groups	ShalySand	0.56	0.39	2.68	23750	0.3
Altena Group	Shale	0.63	0.51	2.72	32500	0.3
Germanic Trias Group	Shale	0.63	0.51	2.72	32500	0.3
Zechstein Group	Shale	unbalanced	unbalanced	2.2	unbalanced	unbalanced

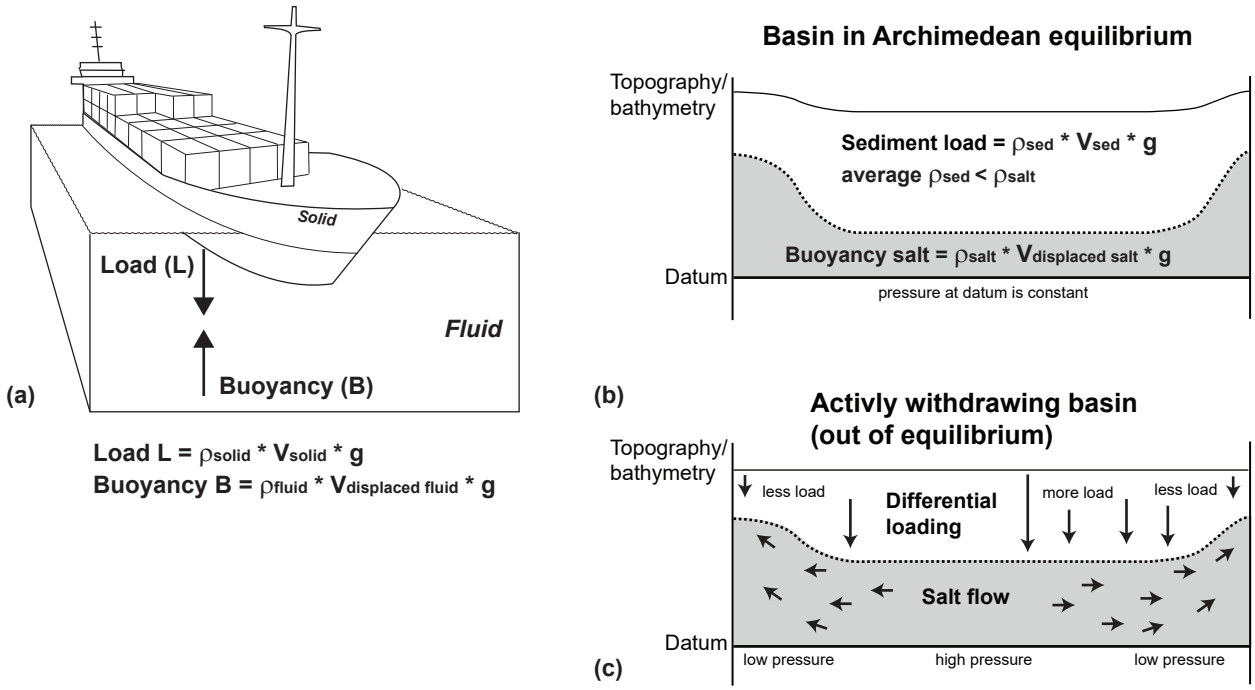

Figure 1. Archimedes' principle. (a) Ship loaded and unloaded floating on water. Buoyancy as upward force exerted by the fluid (water) that opposes the weight of the partially immersed ship. (b) Basin above subsurface evaporites in Achimedean equilibrium. Salt treated as dense pseudo-fluid (= 2.2 g/cm^3) loaded by cumulatively lighter overburden rocks (solid). Backstripping corresponds to incremental unloading of the overburden (sensu Maysternko et al. 2013). Archimedean restoration of the Zechstein Basin example justified by minor/slow subsurface salt flow. c) Basin out of equilibrium by major differential loading with significant salt flow and high differential pressure at datum level.

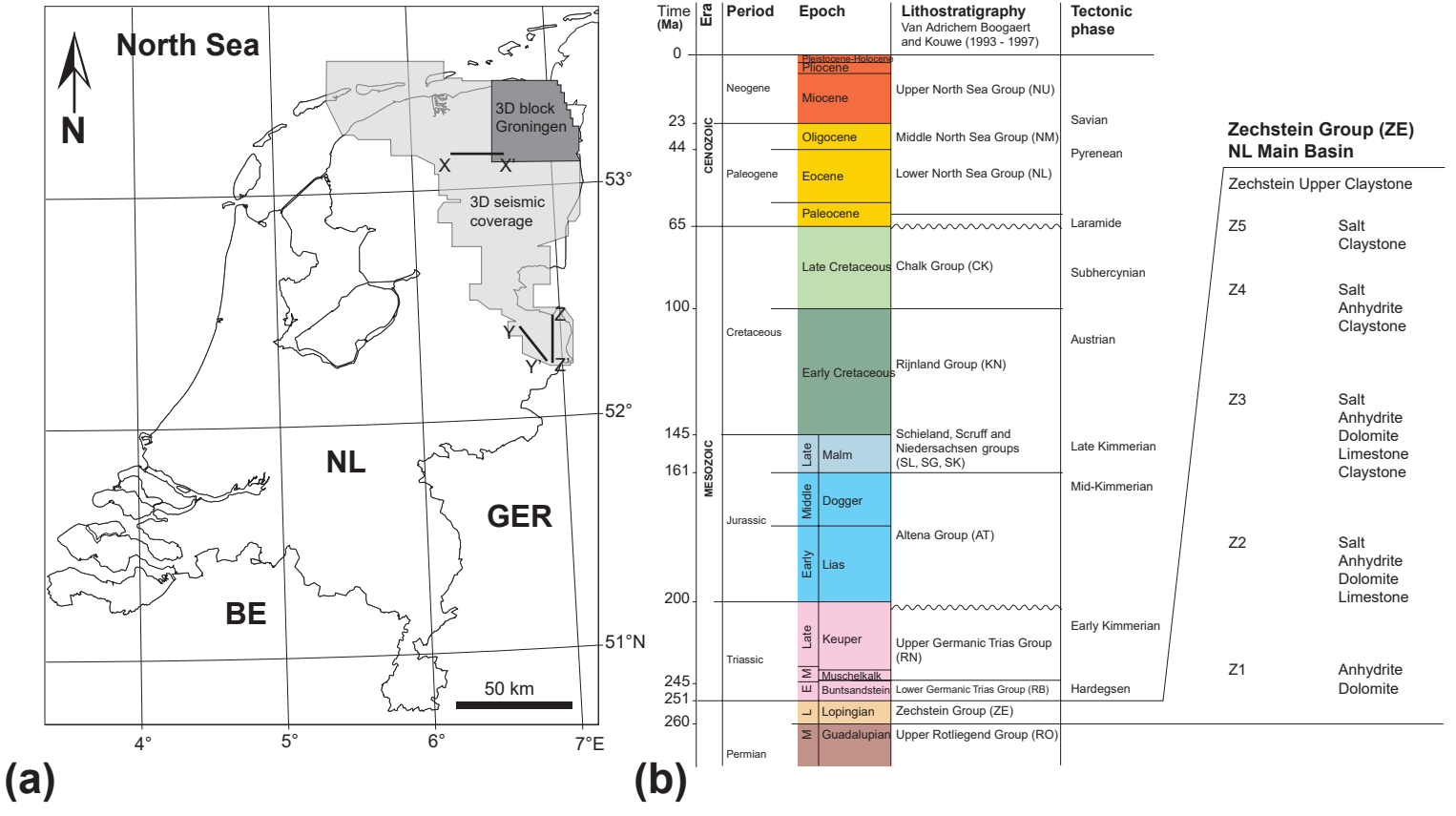

Figure 2. Study area. (a) Study area in the NE of the Netherlands and 3D seismic coverage. 3D block Groningen used for quality control. Lines X-X' and Y-Y' shown on Figure 3. BE = Belgium; GER = Germany; NL = The Netherlands. (b) Stratigraphy of the study area (after Van Adrichem Boogaert and Kouwe, 1993). Detailed lithostratigraphic subdivision of the Zechstein Group on the right. Stratigraphic abbreviations used on following figures.

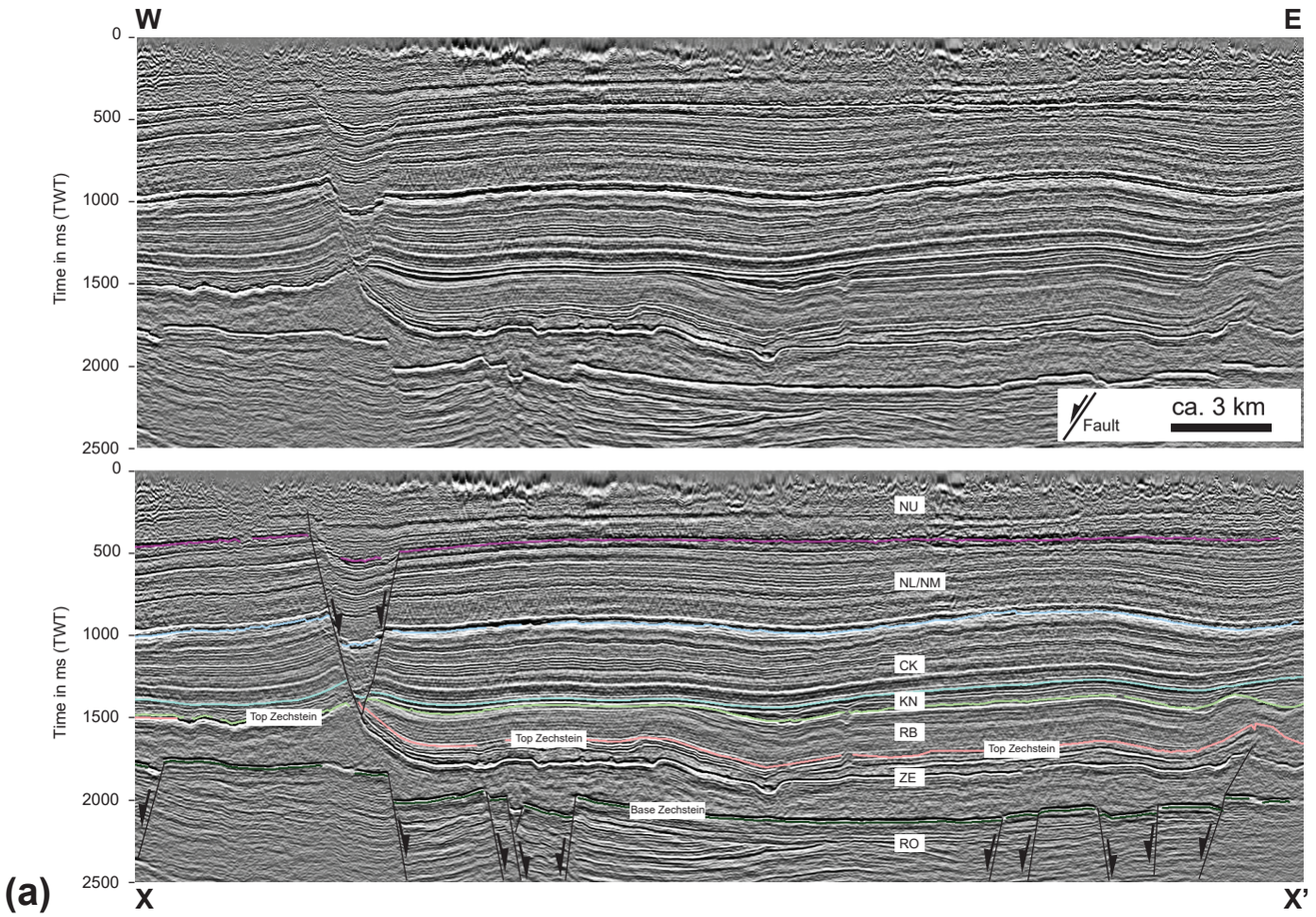

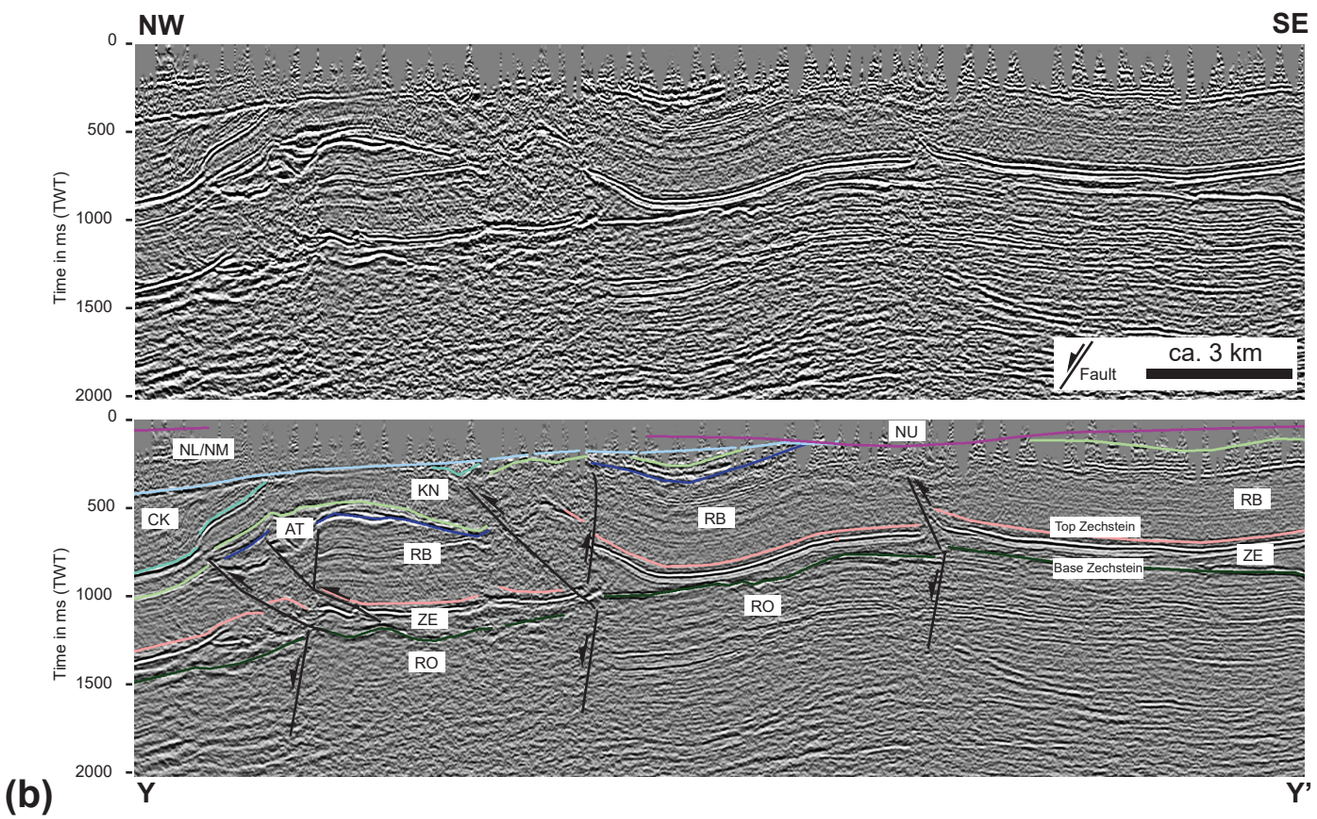

Figure 3. Seismic-reflection data. (a) Seismic-reflection line X-X' across the northern-central study area. Top – uninterpreted, base – interpreted. Note Zechstein unit (ZE) and bright, strong amplitude reflection near top imaging partly deformed and folded intra-salt Zechstein 3 stringer (Strozyk et al., 2012). (b) Seismic-reflection line Y-Y' across southern study area. Top – uninterpreted, base – interpreted. Note lack of upper Mesozoic and Cenozoic Zechstein overburden in the south. For line locations and stratigraphic abbreviations see Figure 2.

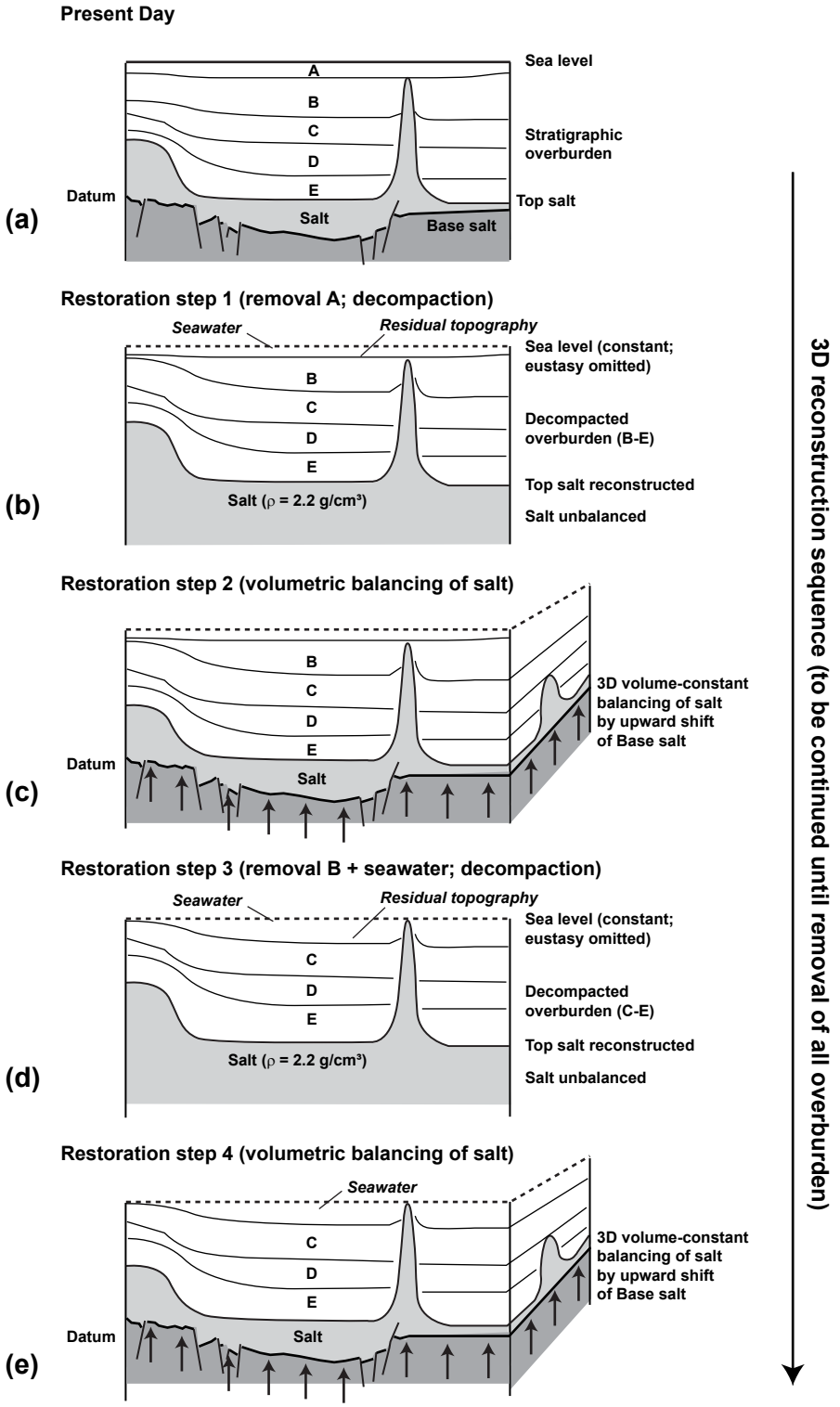

Figure 4: Restoration methodology. (a) Present-day situation. (b) Restoration step 1: Removal of top layer A. Airy-type vertical unloading of sedimentary column down to Top salt. Decompaction of sedimentary column down to Top salt (only restoration scenarios 2 and 3). Salt unit remains unbalanced. Residual topography flooded with seawater. (c) Restoration step 2: Upward vertical shift of unbalanced Base salt into new position constrained by keeping salt volume constant. (d) Same as restoration step 1 but with new top layer B. (e) Same as restoration step 2. Entire 3D unloading procedure to be continued until removal of all salt overburden (see Fig. 5).

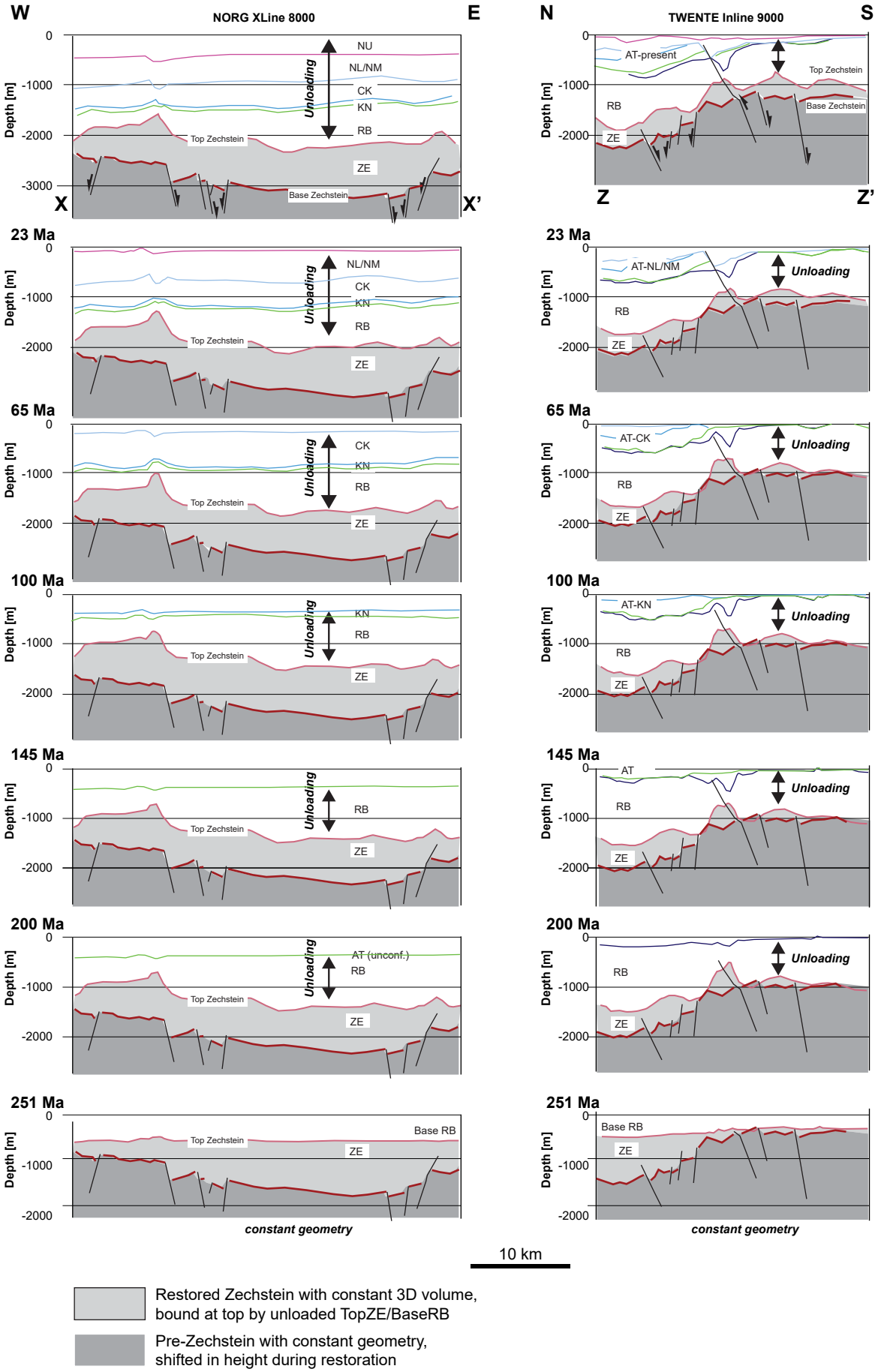

Figure 5: Restoration examples (scenario 2 - unloading and decompaction). Selected geological sections (NORG XL 8000; TWENTE IL 9000) through the 3D restoration that illustrate the sequential evolution of structure, stratigraphy and thickness of the Zechstein unit. Note absence of Jurassic strata (AT unconformity) along cross section X-X' (NORG XL 8000). Also note pronounced flattening of Top salt through time. For illustration of inferred 3D salt thickness change and 3D subsurface salt flow through time see Figures 6 to 8. For location of sections see Figures 2 and 6-10).

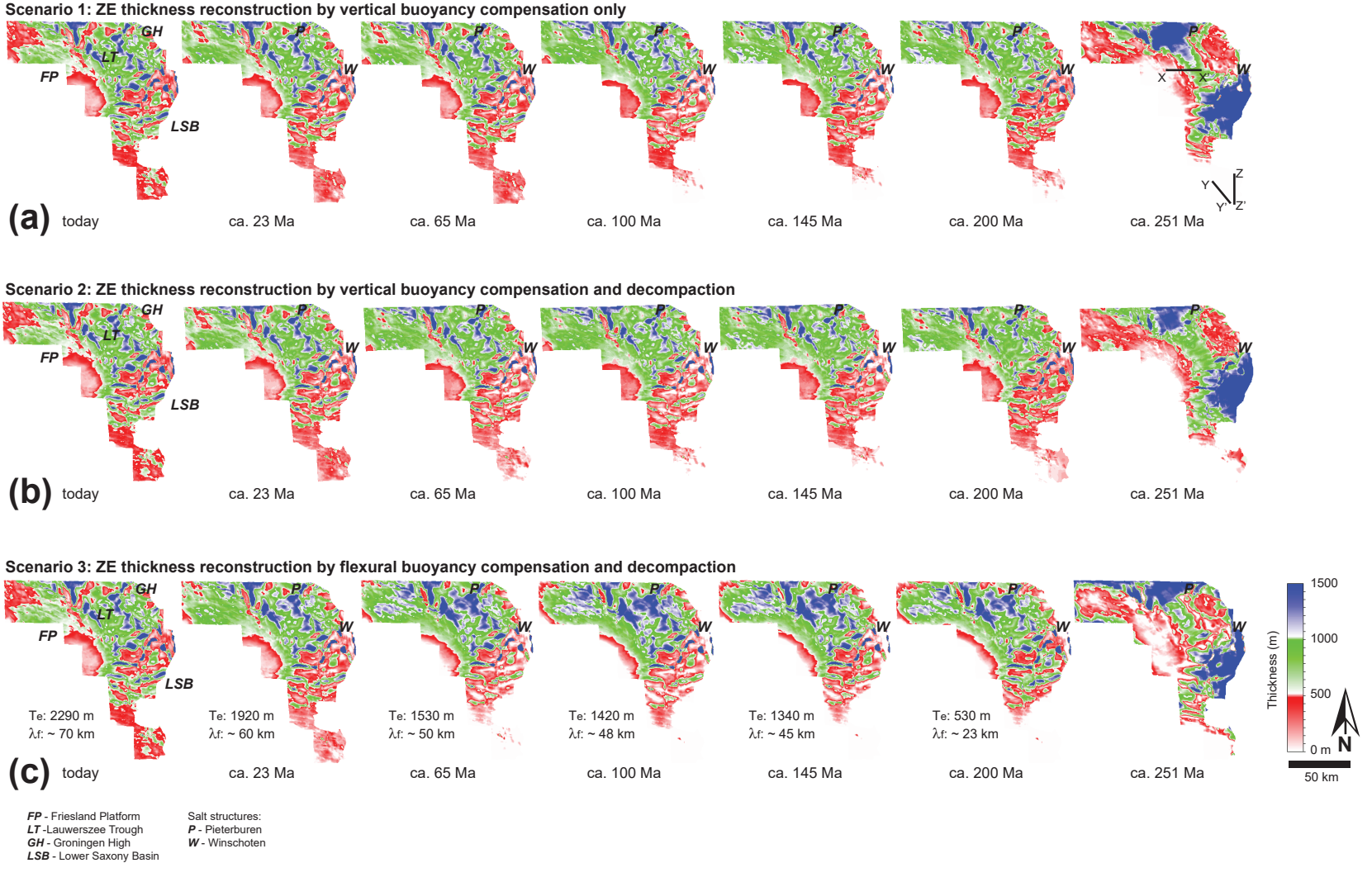

Figure 6. 3D Zechstein thickness-reconstruction results by backstripping. Note 251 Ma thickness maximum of Zechstein in Lower Saxony Basin (LSB) and Lauwerszee Trough (LT) in all reconstructions. (a) Backstripping scenario 1 – restored Zechstein thicknesses by vertical buoyancy compensation ("Airy balancing") omitting decompaction. (b) Backstripping scenario 2 - restored Zechstein thicknesses by vertical buoyancy compensation ("Airy balancing") including decompaction. (c) Backstripping scenario 3 - restored Zechstein thicknesses by flexural buoyancy compensation including decompaction. Effective elastic thickness (Te) of the overburden calculated as average overburden thickness from preceding restoration step; note corresponding change of flexural wavelength (f) during backstripping. All reconstructions using submarine conditions. FP = Friesland Platform; GH = Groningen High; P = Pieterburen; W = Winschoten. 2D restoration (scenario 2) extracted along sections X-X' and Z-Z' shown in Figure 5.

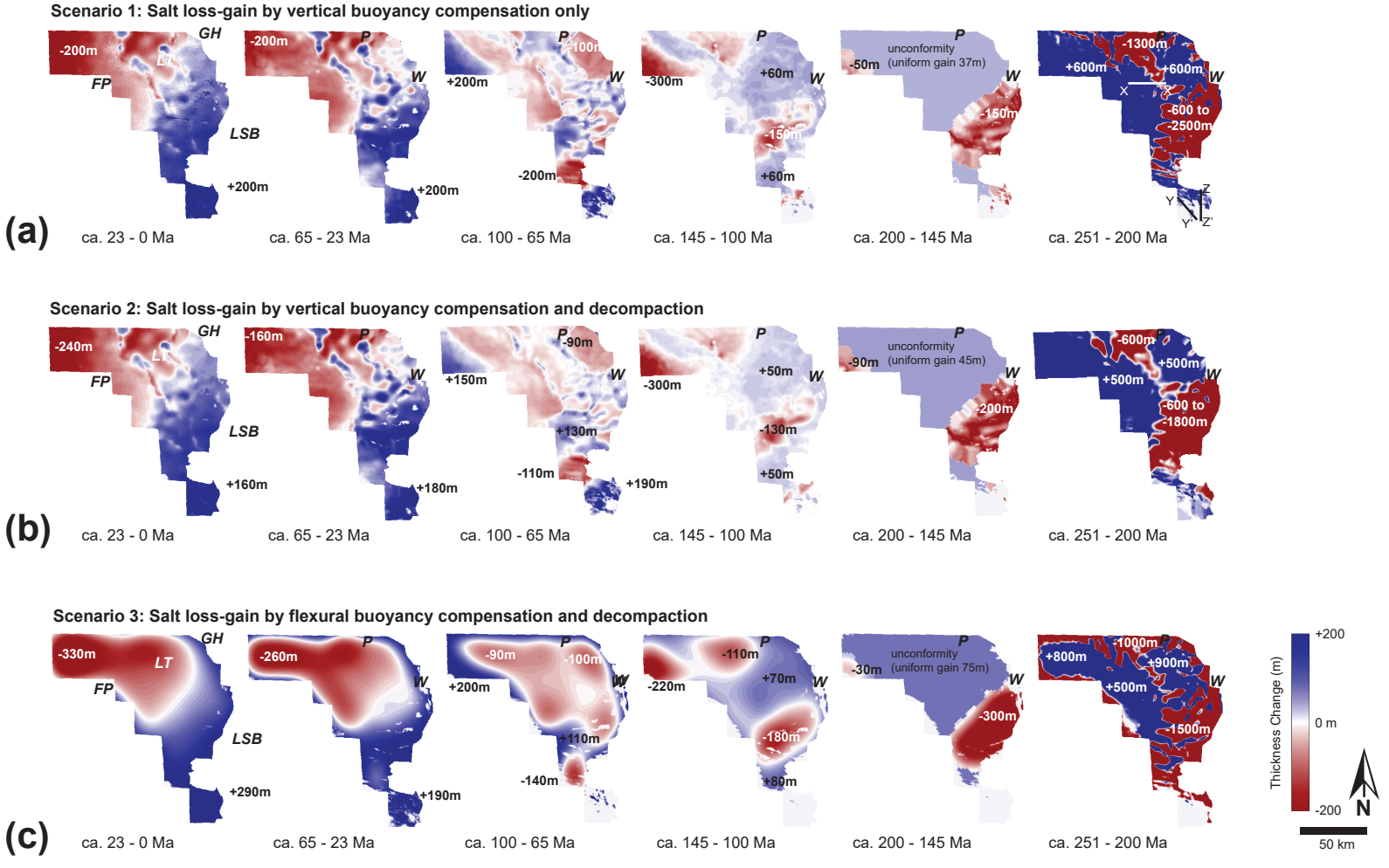

Figure 7: Differences calculated between successive pairs of isopachs of Figure 6. (a) Salt loss-gain plot of backstripping scenario 1. (b) Salt loss-gain plot of backstripping scenario 2. (c) Salt loss-gain plot of backstripping scenario 3. Note similarity between vertical buoyancy compensation of backstripping scenarios 1 and 2 documenting limited significance of decompaction. Note pronounced difference between flexural buoyancy compensation (c) and vertical balancing (a, b) between recent time and the Early Cretaceous (145-100 Ma).

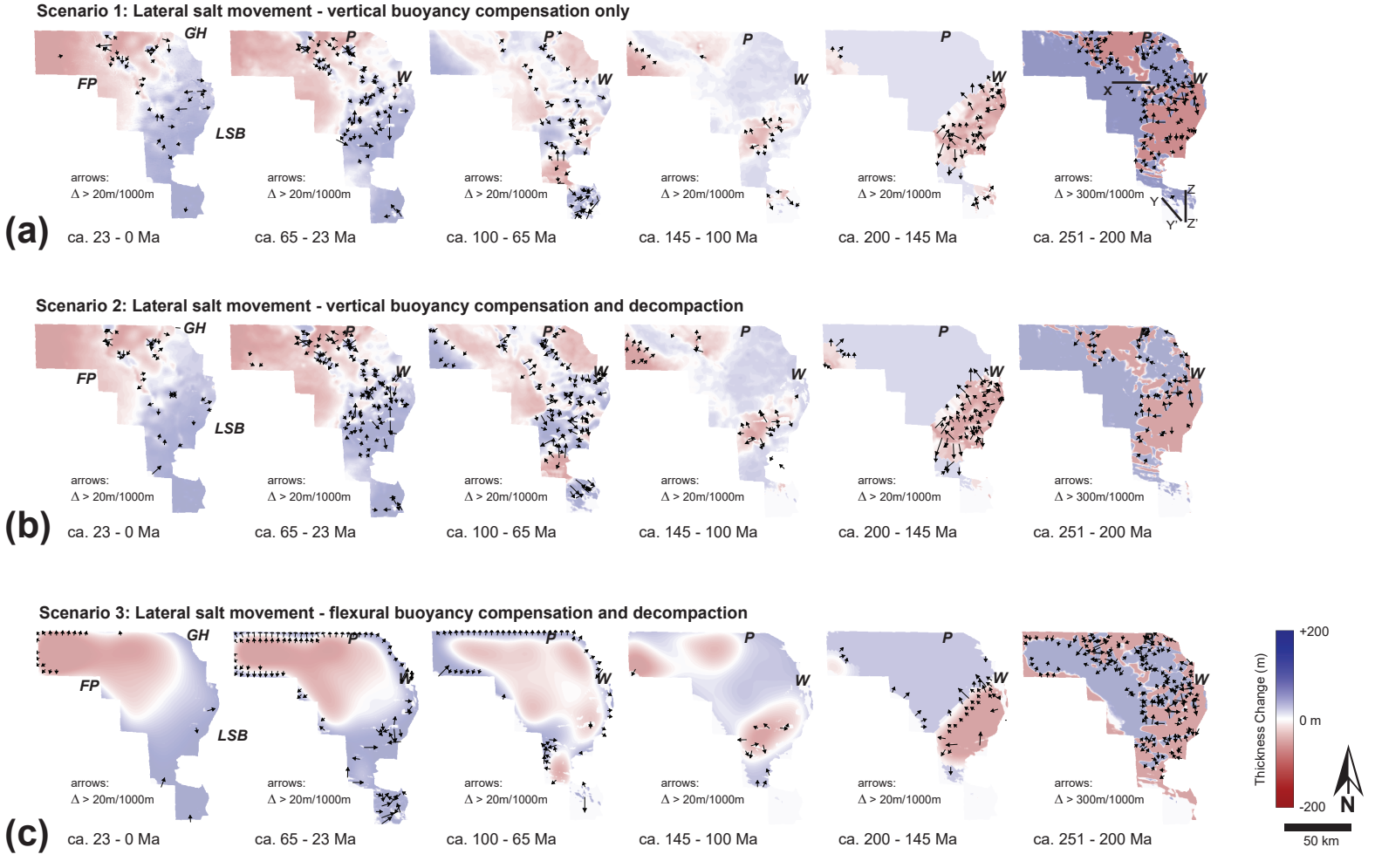

Figure 8: Maximum lateral change derived from difference plots of Figure 7. (a) Orientation of maximum lateral change based on backstripping scenario 1. (b) Orientation of maximum lateral change based on backstripping scenario. (c) Orientation of maximum lateral change based on backstripping scenario 3. Note pronounced edge effects at northern boundary of study area associated with flexural backstripping (scenario 3).

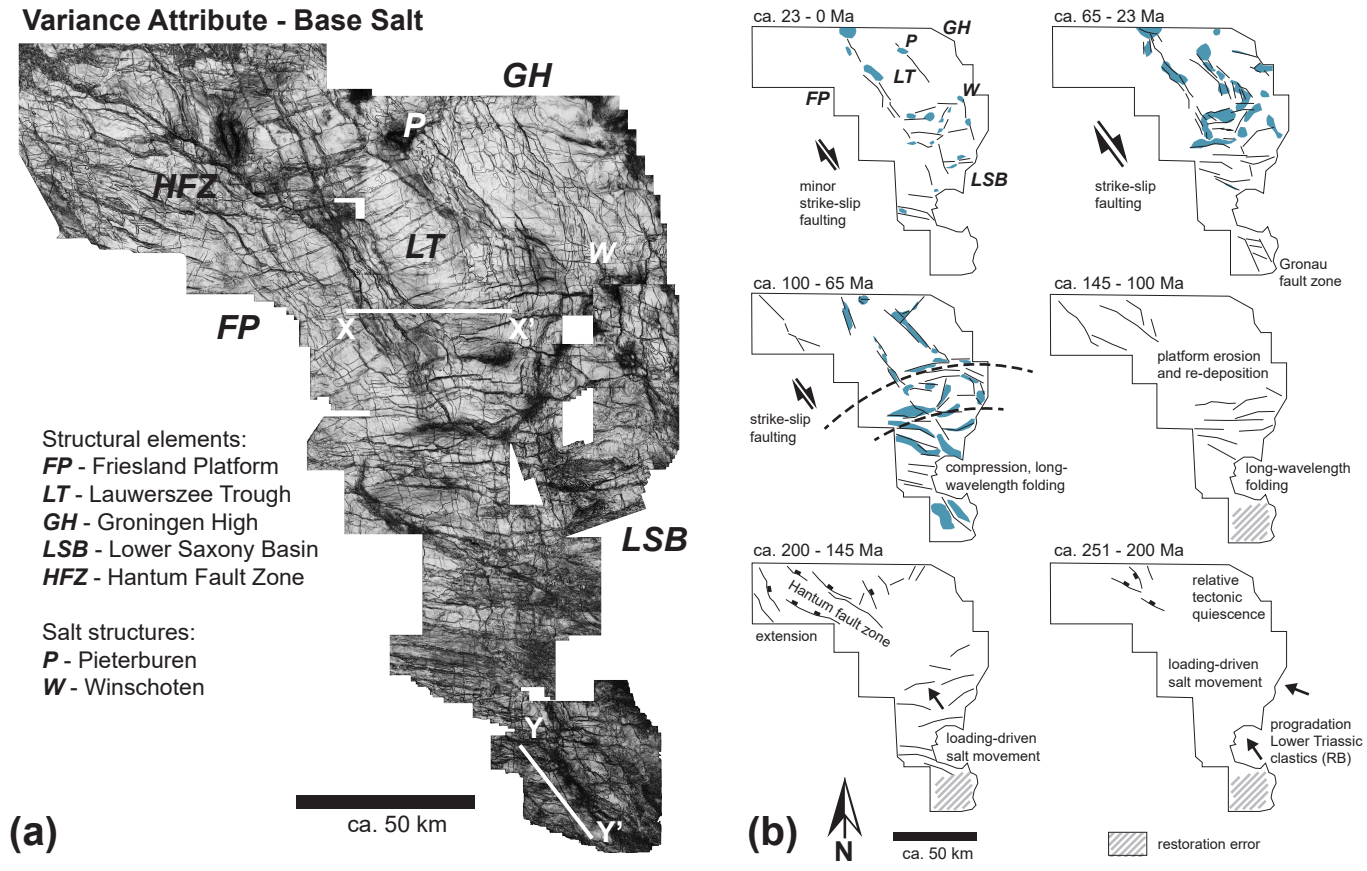

Figure 9. Interaction of tectonic framework and subsurface salt flow. (a) 3D variance horizon-slice highlighting main structures of the pre-Zechstein. Hantum Fault Zone (HFZ) between FP and LT characterized by significant salt gain in the Early Cretaceous. (b) Interpretation of relationship between sedimentary processes, tectonics and subsurface salt movement. Seismic-reflection data along lines X-X' and Y-Y' shown on Figure 3.

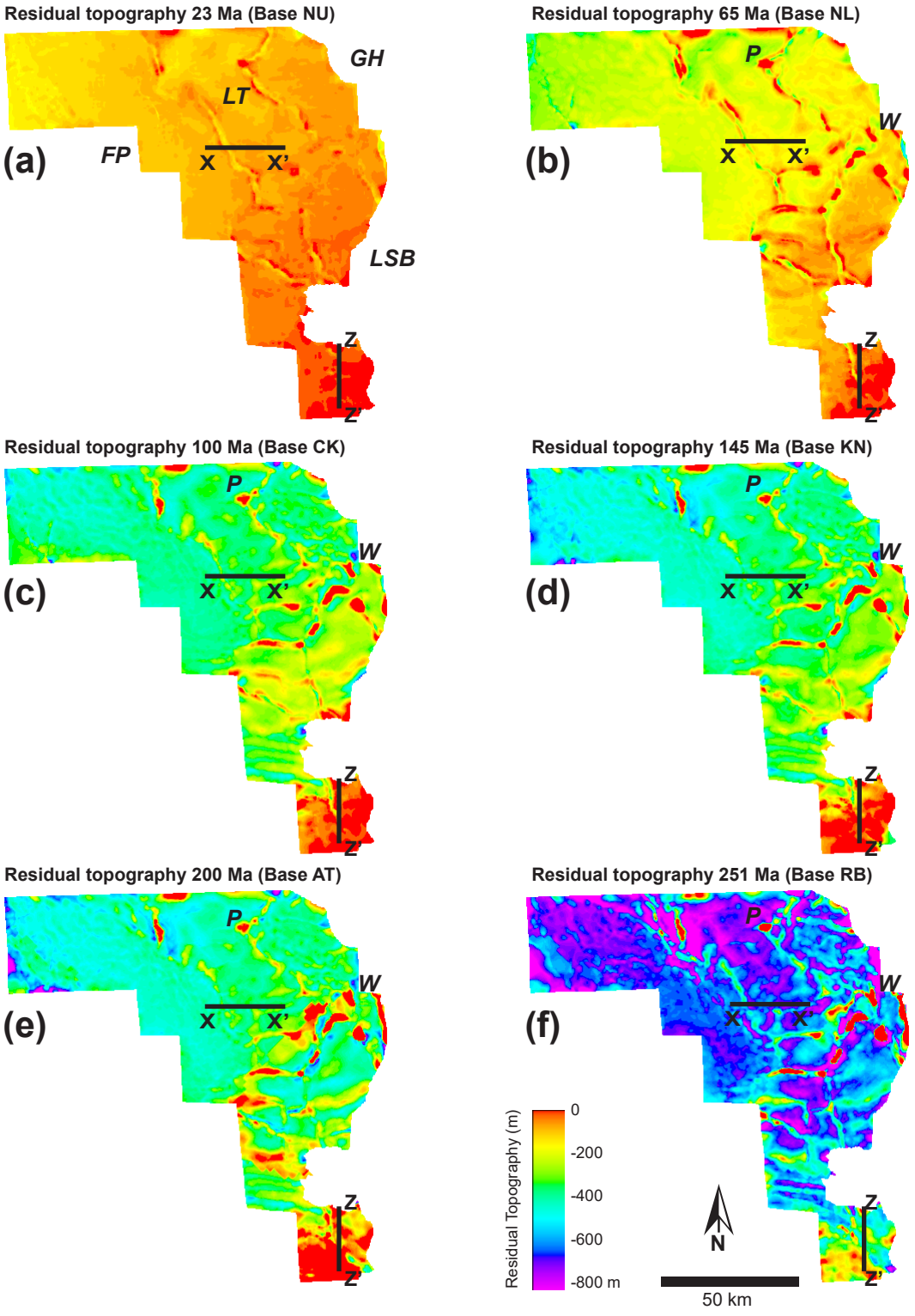

Figure 10: Residual 3D topography (submarine) after each reconstruction step in scenario 2 (unloading and decompaction). Depth position of respective model top at (a) 23Ma; (b) 65Ma; (c) 100Ma; (d) 145Ma; (e) 200Ma; and (f) 251 Ma. Note restoration of increasingly flat basin-floor topographies away from salt diapirs and ridges. Note piercement salt diapirs Pieterburen (P) and Winschoten (W) that remain unbalanced thoughout restoration.

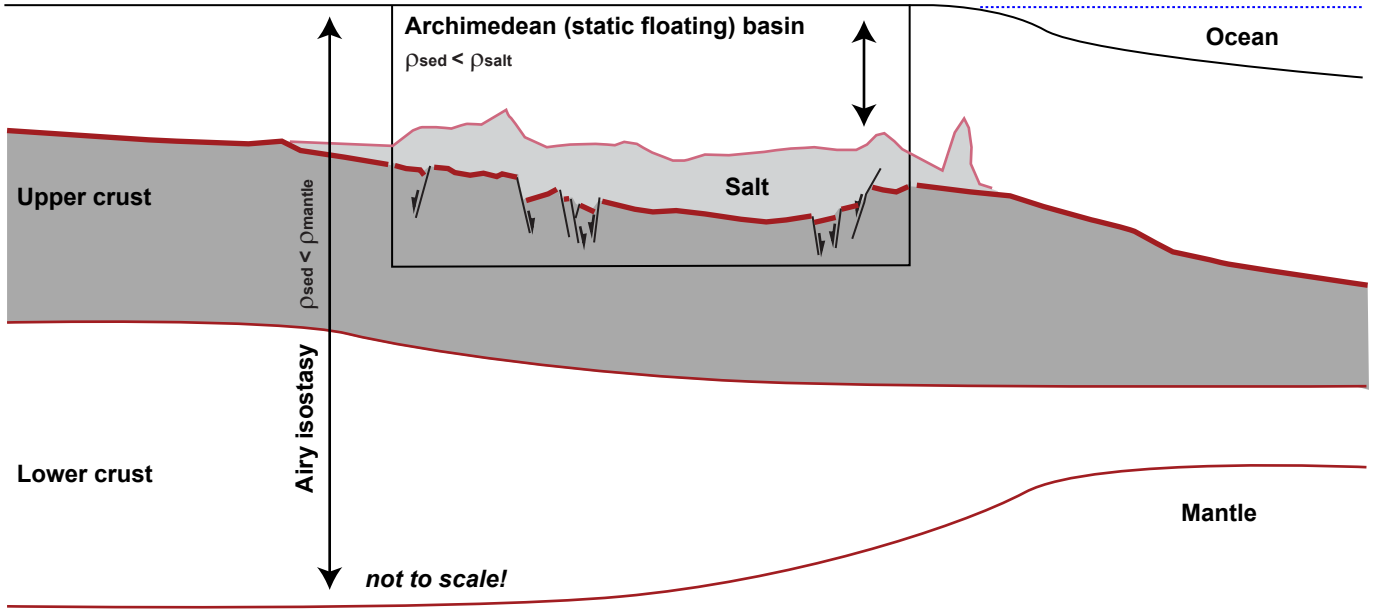

Figure 11: Scale and scope of the salt-restoration of this study in comparison to "classic" crustal-scale backstripping (e.g. Turcotte and Schubert, 2014). The concept of isostatic correction is essentially the same for calculating the total mass above a reference datum i) at great depth below the base of the crust; or ii) at Top salt, ignoring everything that happens below that level. Note that volumetrics, lateral distribution, thickness, state of aggregation and physical properties of the respective reconstruction base (salt/evaporites versus the Earth's mantle) are yet fundamentally different.